Prospects and Challenges of Inertia Emulation Methods for Low Inertia Power Systems

Muhammad F. Umar, Amirhosein Gohari Nazari, Mohammad B. Shadmand Dept. of Electrical & Computer Engineering, University of Illinois Chicago, IL, USA mumar6@uic.edu, agohar2@uic.edu, shadmand@uic.edu

Abstract— Due to massive incorporation of the renewable energy resources into the upcoming power grid, the share of power generation from synchronous generator (SG) is being decreased and is being replaced by distribution generation (DG). This change has led the significant decrease in the overall power system's inertia and transforming the future power system into low inertia power systems (LIPS). Because of the huge rotational mass of SG, it intrinsically provides system inertia that is critical for the stable and resilient operation of the power system under different types of disturbances. To cope with the challenges of stable operation of LIPS, several inertia emulation schemes has been proposed in the previous literature. However, each scheme has its specific benefits, limitations, and applications. Thus, this paper provides a comprehensive insight to the inertia emulation schemes for DG and compares each scheme in terms of implementation challenges and experimental effectiveness in enhancing the overall system's inertia. Moreover, this comparison is supported with experimental results and analysis to validate virtual inertia emulation schemes.

Keywords— Inverter based generation, Low inertia power system, emulation of virtual inertia, renewable energy.

I. INTRODUCTION

The global vision of deploying significantly higher amount of renewable energy to achieve net-zero emissions from power sector is transforming the existing power system from centralized generation to more distributed generation (DG) based grid. The key DG resources includes solar energy, wind energy, fuel cells, etc. [1]. In 2022, the global capacity of the renewable energy-based generation reached to 3372 GWs. Out of which solar energy shares 1053 GWs, and wind energy accounted for 899 GWs [2]. By the end of 2023, the expected global generation from renewable energy resources will exceeds 4000 GWs and this will be majorly dominated with solar generation. Moreover, it is expected that solar based generation is going to rise to 1160 GWs and wind energy's share will be 992 GWs in distributed generation [3]. Thus, these projected figures for growth of renewable energy integrated with the existing power grid indicate that the synchronous generator (SG) based centralized generation is being displaced by DG based on renewable energy. In most cases, a power electronics interface such as an inverter is required to integrate these DG sources with the power grid. Therefore, the future power system is evolving into a new energy paradigm within smart grid concept. In this concept the foremost generation will be from the power electronics-based converters thus, future power grid will be dominated with the converter-interfaced DG.

Fig. 1 Illustrates this inertia concept with aid of mechanical spring system for the upcoming power system. The prime

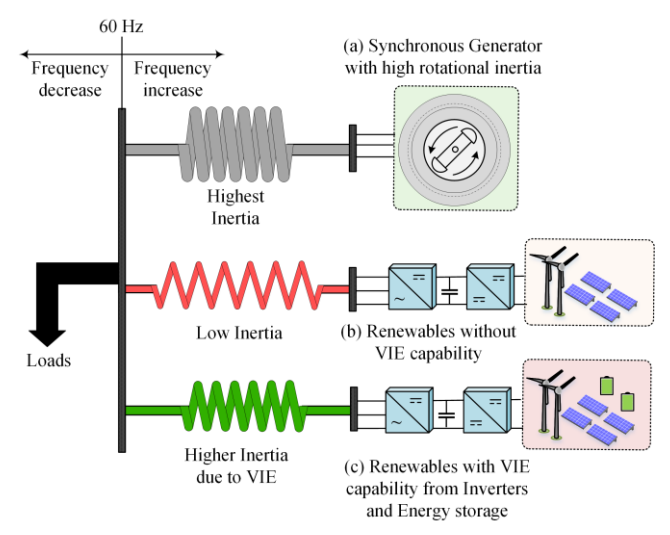


Fig. 1. The concept of inertia in upcoming power systems is depicted with help of mechanical spring system: (a) SGs with stiff and strong spring referred as highest inertia contributor, (b) Renewables without VIE considered as the loose spring with low inertia contribution, (c) Renewables with VIE via smart inverters and energy storage are depicted with relatively stiffer spring that have higher inertia support.

source of generation in upcoming power system are power electronics-based converters, so the number of SGs in upcoming power grid will be substantially smaller. Therefore, the inherit rotational inertia from SGs that is critical for stable and resilient operation of the power system will be significantly less and this leads to the emergence of low inertia power system (LIPS). According to the North American Electricity Reliability Corporation (NERC) report published in 2017 [4], the overall system inertia of the eastern interconnection of USA is on decreasing trend due to displacement of SGs based generation with DG based on renewable energy. Fig.2 illustrates the interconnection frequency response obligation (IFRO) to disturbance between year 1994 to 2022. The frequency response of eastern interconnection is on decline between the observed years. IFRO is referred as the minimum amount of the frequency response that must be maintained by the interconnection. The initial frequency response of the power system is directly related to the overall system's inertia. Thus, evolution of the existing power system into LIPS is inevitable in coming years.

Several challenges are reported in the existing literature for the stable operation of LIPS. One of the most critical issues in LIPS is the frequency stability. According to the swing equation, system frequency is directly related to the balance between mechanical input power and electrical load output power. Any slight unbalance between input power and demanded power can cause deviations in the system frequency. In LIPS, due to lower rotational inertia, changes in the frequency is more drastic because of grid disturbances such as addition of a load, loss of generation, etc. [5, 6]. Moreover, frequency nadir will fall to a lower point in LIPS as compared to power system that has higher inertia [7]. Another critical challenge for stable operation LIPS is the rotor angle stability. The acceleration of the rotor angle can occur due to unbalance in the swing equation. The rotor angle stability is categorized by small signal stability and large-signal or transient stability. The sensitivity analysis is applied in [8] to determine the effect of uncertainty in the generation under high amount of intermittent renewable energy resources integration. This work concluded that reduced system inertia and intermittency leads to reduced dampening of critical system states and thus, affecting small signal stability of interconnected power grids. Under large-scale disturbances in LIPS, the rotor angle may face sudden large acceleration and that can lead to loss of synchronism [9] which can take the generation unit out of the grid.

These adverse effects on the stability of LIPS can be mitigated via emulation of inertia from the power-electronics converters [10]. Specifically, the controller structure of converter can be modified to enhance the frequency response during disturbance, and hence, increasing overall system's net inertia. The existing inertia emulation methods includes emulating SG's dynamics by adopting the swing equation in the primary control of the power electronics converter. This type of converter control is known as virtual synchronous generator control [11]. Moreover, the droop-controlled grid forming inverters can also be manipulated to enhance the system's inertia [12]. Furthermore, system inertia can also be boosted by emulating the inertia via battery energy system [13], DC link capacitors [14], flywheels [15], etc. Thus, this paper provides a comprehensive review on the inertia emulation techniques and compares the performance and application of each scheme. The effectiveness of inertia emulation from different control structures of inverter is validated via hardware experimental tests which is not very well studied nor compared in the

The remaining part of the paper is divided as, section II discusses in detail stability issues and challenges in LIPS, section III provides a comprehensive review of the inertia emulation schemes for LIPS. An experimental case study to compare various inertia emulation schemes is presented in section IV. Finally, conclusion of the work is presented in the section V.

II. STABILITY CHALLENEGES IN LIPS

Inertia is defined as the ability of a physical body with mass to resist to change. If the body is in state of motion, it will remain in state of constant motion until applied an external force to accelerate or deaccelerate. Bulkier the body is, more resistance it provides to change under the disturbance created

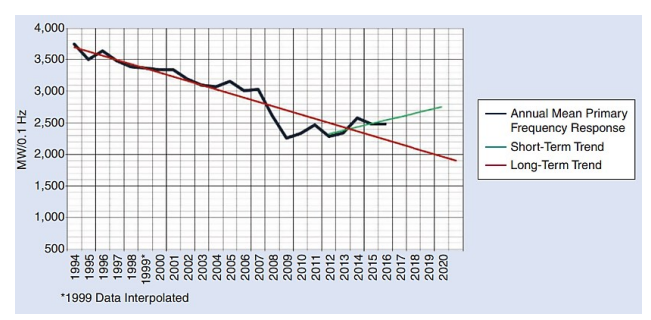


Fig. 2. Decreasing trend of IFRO from the eastern interconnection according to NERC report 2017 [4].

by external forces. In the conventional bulky power system, SGs, turbines, and induction generators are the huge, massive rotating bodies and these rotating masses have a strong coupling with the grid and have an ability to store the kinetic energy. This stored kinetic energy in rotational reference frame is directly related to the moment of inertia and square of angular velocity. Therefore, during the disturbances in power system such as addition of huge loads, loss of generators, etc. the conventional power system has a capability to provide critical inertia required to maintain frequency stability and rotor angle stability. However, in LIPS major part of generation is from DG interfaced with the power electronics converters that can't provide the rotational inertia like SGs. Moreover, the intermittent nature of renewable energy such as solar and wind energy bring uncertainty in the total generation of a power system. Thus, it can easily disturb the load-generation balance of a power system, and it can disrupt frequency stability and rotor angle stability.

A. Frequency instability in LIPS

The stability of the power system's frequency is linked with maintaining the supply and demand balance or in other words all the time meeting load demand with power generation from the power system. The goal of power system control operator is to maintain a constant value of the system frequency around nominal value of 50 Hz or 60 Hz. Small deviations from the nominal frequency can cause catastrophic tripping and system failures [16]. Therefore, the frequency stability is fundamental rule for the stable operation of a power system. The frequency dynamics of a generation source are dictated by the swing equation given as,

$$\frac{d\omega_g}{dt} = \frac{T_m - T_e - Dp\Delta\omega}{J} \tag{1}$$

where J is the rotational inertia constant, ω_g is the grid frequency, T_m and T_e are the mechanical torque provided by generation source and electrical torque exerted by the load, D_p is the damping constant and $\Delta\omega$ refers to the change in the frequency. It can be seen from (1) that any small changes in electrical torque exerted by the load or in mechanical torque generated via generation source can directly trigger the change in the frequency and determine the rate of change of frequency (RoCoF). However, if the inertia constant has bigger value, these changes in the frequency can be minimized and resultantly, the RoCoF becomes smaller. In LIPS as SG-based inertia is low, thus the risk of high frequency deviations from

the nominal value due to the load disturbances or generation loss is much higher. Another reason for the frequency instability is the poor power sharing between DGs in LIPS. This can trigger small perturbations in system's frequency that can last from seconds to minutes [17]. To mitigate these frequency deviations often the DG are equipped with a secondary level of control that can restore the nominal frequency and is often operating at much slower timescale than the primary controller. Thus, if the frequency remains at lower value than nominal value for longer time due to the slower frequency restoration control dynamics, it can trigger unnecessary tripping of the protection relays in power system that results in a blackout. Therefore, the frequency instability issue in LIPS is one of the critical challenge to be solved in upcoming power grid.

B. Rotor Angle instability in LIPS

The rotor angle stability of a generator is defined as the ability of the connected generation sources to remain synchronized to the power system under disturbance and in post-disturbance state. In more details, if the rotor angle of SG remains synchronized to the power grid during the disturbance (small and large-scale) and return to the original equilibrium point or a find new equilibrium point that is less than the critical angle in the post-disturbance condition, then this SG will not experience the rotor angle instability issue. Typically, rotor angle stability is assessed in two categories, small-signal stability and large-signal stability or transient stability. The small signal stability of LIPS is assessed via linearizing the state-space model of the given system and then small perturbations are applied to this model to derive critical eigenvalues. The work [18] discusses the small-signal stability of LIPS comprised of two different types of grid-forming inverters and concluded that due to the differences in the controller implementation, both inverters have different dynamics during the perturbation that can impact the smallsignal stability of a microgrid. On the other hand, the largesignal stability is related to the stability of rotor angle and ability of the connected generation sources (either SG or converter-based generation) to maintain synchronism with other connected generators after the large-scale disturbance such as faults, large loads and sudden loss of a bulky generation unit. In LIPS the generation sources are dominated with the DG source based on inverters and a small portion of SGs. Thus, the mismatch between two types of generation sources can cause multiple types of loss of synchronism (LOS) between SGs and inverters during the large-scale disturbances [19]. Moreover, dynamic interactions during the disturbance between different inverters-based DG sources in LIPS are intensified due to its low-inertia characteristic and this interaction can have adverse effects upon the large-signal rotor angle stability of LIPS.

III. INERTIA EMULATION SCHEMES FOR LIPS

To address the stability challenges in LIPS, it requires the inertia emulation scheme to be incorporated with the DGs that can enhance the system inertia. The inertia emulation schemes include direct and indirect methods to enhance inertia of LIPS. For instance, the control of a converter is leveraged to emulate the virtual inertia, power reserve control schemes can be implemented to provide the fast response to the disturbance that enhance the inertia response, battery sources can be interfaced to provide fast frequency response and inertia support, mechanical rotating devices such as flywheel can be installed to boost the inertia. Many other schemes are discussed and compared in this section that provide insights to the inertia emulation for LIPS.

A. Virtual Inertia emulation from grid-forming control of

The DGs that are controlled in the grid-forming (GFM) mode of operation act mainly to regulate the grid frequency and grid AC bus voltage. The GFM control can be developed in various structures that can contribute direct and indirect virtual inertia emulation (VIE). Synchronverter is a topology of GFM control in which the DG is controlled to emulate the dynamics of a SG. This is done by incorporating the swing equation in the control loop of the synchronverter. Fig. 3 (a) illustrates the control architecture of the of the synchronverter [11]. The frequency and voltage magnitude references of the GFM is given by.

$$J\frac{d\omega_{g}}{dt} = T_{m} - T_{ef} - D_{k}(\omega_{0} - \omega_{g})$$

$$\frac{d\theta_{ref}}{dt} = \omega_{g}$$

$$K\frac{d\varphi_{f}}{dt} = Q_{0} - Q_{f} + D_{q}(v_{0} - v_{pcc})$$

$$(2)$$

$$(3)$$

$$\frac{d\theta_{ref}}{dt} = \omega_g \tag{3}$$

$$K\frac{d\varphi_{f}}{dt} = Q_{0} - Q_{f} + D_{q}(v_{0} - v_{pcc})$$
 (4)

where, J is the rotational inertia coefficient, T_m and T_{ef} are the mechanical torque and electrical torque, D_k is the damping constant, ω_g and ω_o are the rotational frequency and reference rotational frequency, respectively. θ_{ref} is the power angle. φ_f is the excitation flux, K is flux control constant, Q_0 and Q_f are the nominal and generated reactive power, D_q is the gain related to the reactive power regulation loop, v_o and v_{pcc} are the nominal voltage and point of common coupling voltage, respectively. Virtual synchronous generator is another control topology of GFM that implements the swing equation in terms of active power rather than torque [20] (see Fig. 3 (b)). The control equations of the VSG are given as,

$$J\frac{d\omega_{ref}}{dt} = P_0 - P_m - k_w(\omega_g - \omega_0) - D_k(\omega_{ref} - \omega_0)$$

$$v_{ref} = D_q \frac{\omega_c}{s + \omega_c} (Q_0 - Q_m) + v_0$$
(5)

$$v_{ref} = D_q \frac{\omega_c}{s + \omega_c} (Q_0 - Q_m) + v_0 \tag{6}$$

where P_0 and P_m are the nominal and measured active power, k_w is the constant of frequency governor, v_{ref} is the generated reference for the voltage magnitude, and ω_c is the cut-off frequency of the low-pass filter. The synchronverter and VSG control for GFM allows the inertia constant to be accessible directly and is given by,

$$H = \frac{J\omega_0^2}{2S_{rated}} \tag{7}$$

where, H is the inertia constant in p.u, S_{rated} is the total rated apparent power of the inverter. Thus, H can be adjusted accordingly for VIE. However, synchronverter and VSG requires a phase-locked loop (PLL) to perform initial synchronization. Therefore, operation of the synchronverter during the severe disturbances or in weak grid is compromised as the performance of the PLL deteriorates under these conditions [21]. An improved implementation of the synchronverter is discussed in [22], this allows the selfsynchronization of the synchronverter during the grid connected operation and improved performance in the islanded operation is reported. Moreover, the VSG suffers from the oscillations in active power and frequency in the multi-VSG based grid during the heavy load disturbances. The dynamics of the VSG is shaped via damping constant and inertia constant. Moreover, designing these parameters to avoid active power and frequency oscillations can mitigate these oscillations [23, 24]. Additionally, adaptive control schemes are utilized to dampen the power-frequency oscillations in the multi-VSG based grid. An adaptive virtual inertia and customized damping constant based scheme is proposed in [25] to improve the stability of the system during the active power oscillations and frequency excursions.

The droop-based control of GFM is another control approach as shown in the Fig. 3 (c). The reference frequency and voltage magnitude for the droop-based control are given by,

$$\omega_{ref} = m_p \frac{\omega_c}{s + \omega_c} (P_0 - P_m) + \omega_0 \tag{8}$$

$$v_{ref} = n_q \frac{\omega_c}{s + \omega_c} (Q_0 - Q_m) + v_0 \tag{9}$$

where m_p and n_q are the droop gains related to the active power-frequency loop and reactive power-voltage loop, respectively. In the droop-based control of GFM inverters, the low-pass filter and droop gain related to the active power-frequency control loop can be adjusted for VIE. Due to the equivalence of the SG and droop proved in [26, 27], the inertia constant is given by,

$$H = \frac{1}{2m_p \omega_c} \; ; \; D_k m_p = 1 \tag{10}$$

VIE in the droop-based GFM can't be controlled in direct manner and it depends upon the combination of both droop gain and the cut-off frequency of a low-pass filter. Therefore, leverage of independently controlling the system's inertia for the droop based GFM is limited [28]. Moreover, the droop based GFM control has reported issues of small signal instability due to the cross-coupled terms, active power, and voltage (P-V) and reactive power and frequency (Q-f) in the high resistive network [29]. The solution to this challenge is to incorporate virtual impedance that modify the network's impedance to be more inductive in nature and decouple the real and reactive powers [30]. Moreover, sub-nominal frequency and voltage levels in the steady-state conditions after the disturbance is reported. A secondary controller is required to restore the frequency and voltage to the nominal levels in steady-state conditions [31]. Like the droop control, the powersynchronization control (PSC) of GFM have a capability of the VIE [32]. As depicted in the Fig. 3 (d), the structure of the PSC of GFM. The subsystem is mathematically modelled as,

$$\theta_{ref} = \frac{1}{s} \left(k_p \frac{\omega_c}{s + \omega_c} (P_0 - P_m) \right) + \theta_g \tag{11}$$

where, θ_{ref} is the reference voltage angle of GFM, θ_g is the grid voltage angle, k_p is the PSC gain. It is revealed from comparing (5) and (11) that relation for the inertia emulation can be derived [33]. This relation is given by,

$$H = \frac{\omega_c}{2k_p S_{rated}} \; ; \; D_k = 0 \tag{12}$$

The superiority of the PSC control over the other GFM control scheme is that it doesn't rely on the dedicated synchronization

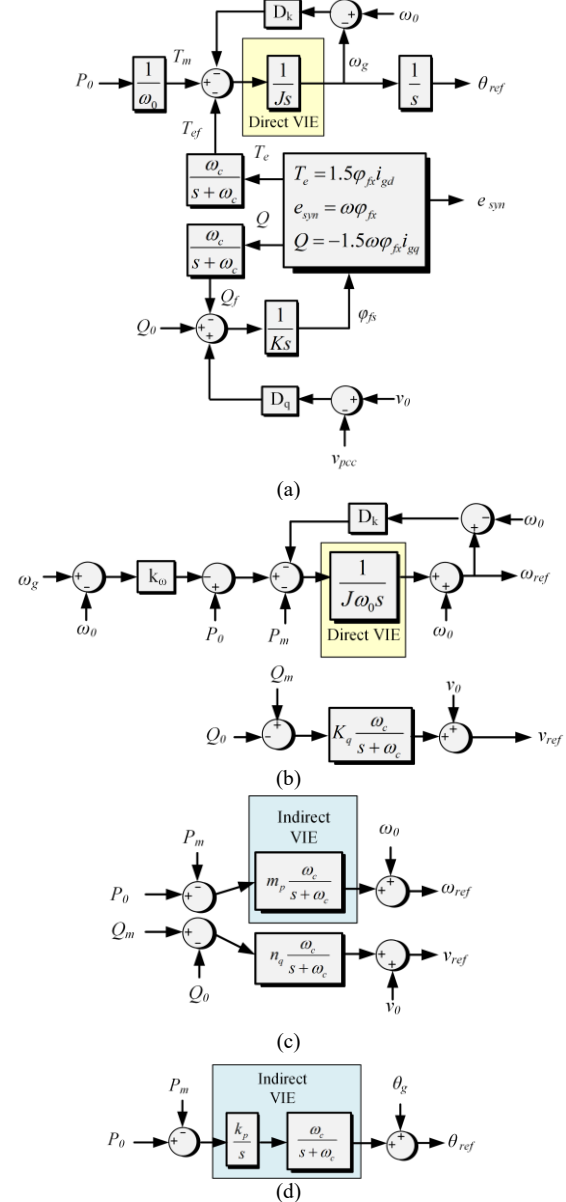


Fig. 3. Comparison of GFM control schemes for the virtual inertia emulation: (a) Synchronverter, (b) Virtual synchronous generator, (b) Droop control, (d) Power synchronization control.

unit and the active power can be seamlessly synced with the grid [34]. However, a backup PLL is required to operate during the large-scale disturbances such as faults.

B. Virtual Inertia emulation from grid-following control of DGs

The grid-following (GFL) mode of operation requires the DGs to act in current-controlled mode and sink the active and reactive power into the grid. The GFL control require to detect the grid's angle and it is detected via PLL. A simple implementation of the PLL is depicted in Fig, 4 (a) and the related transfer function of this PLL is given by,

$$\frac{\theta_g(s)}{v_{gg}(s)} = \frac{k_{p-PLL}s + k_{i-PLL}}{s^2 + k_{p-PLL}s + k_{i-PLL}} = \frac{2\xi\omega_n s + \omega_n^2}{s^2 + 2\xi\omega_n s + \omega_n^2}$$
(13)

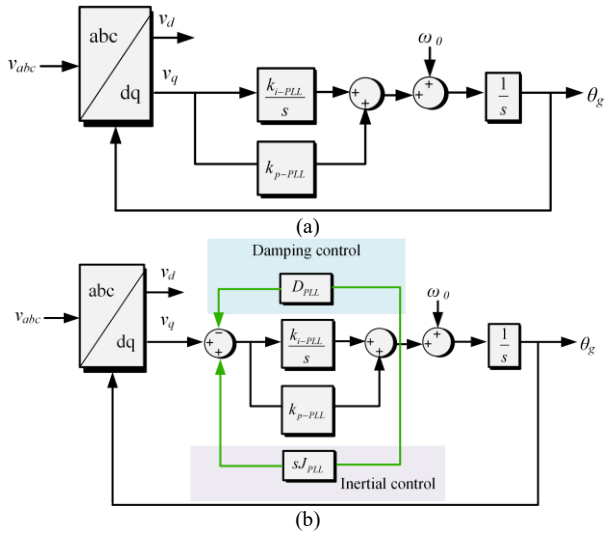


Fig. 4. PLL based GFL control scheme for the virtual inertia emulation: (a) Conventional PLL, (b) Inertial PLL

where, $k_{p\text{-}PLL}$ and $k_{i\text{-}PLL}$ are the gains for the PI controller incorporated in the PLL. θ_g is the grid voltage angle and v_{gq} is the quadrature component of the grid voltage. ω_n is referred as the undamped natural frequency, and ξ is the damping ratio. To incorporate the inertial effect in PLL, the conventional PLL structure is compared with the SG model and then modified as illustrated in the Fig. 4 (b). The equivalent inertia constant and the damping constant [35] can be calculated based on the control designer's requirement and the mathematical form of these parameters are given as,

$$J_{PLL} = \frac{1}{\omega_n^2} ; D_{PLL} = \frac{2\xi}{\omega_n}$$
 (14)

where, J_{PLL} and D_{PLL} are the inertia constant and damping constant for the PLL. In the inertial PLL, the VIE can be implemented by directly increasing the value of the J_{PLL} , however, if a very large J_{PLL} is selected it will result in the bandwidth reduction and this leads to the slower response of PLL [36]. Another method for the VIE from GFL control is to implement the power reserve module (PRM). Conventionally the photovoltaic (PV) interfaced GFL inverters are operated at the maximum power point (MPP) to deliver the maximum harvested power to the connected grid. However, the PRM operate GFL inverters at the non-MPP and keep some portion of the active power as a reserve. This power reserve can be used in the events when the frequency support is required and the GFL inverter can swiftly inject this reserve power to improve frequency response to the grid disturbances. The relation between the inertia constant for VIE provided via PRM [37] is given as,

$$H = \frac{P_{reserve} / P_{rated}}{2 \frac{d\omega}{dt} / \omega_0}$$
 (15)

where, $P_{reserve}$ is the active power reserve of the GFL and P_{rated} is the rated power of the PV module. Due to the fast-acting GFL to deliver the required active power to support the frequency, this scheme for the VIE is highly effective. However, finding the exact value of power reserve and maintaining the balance

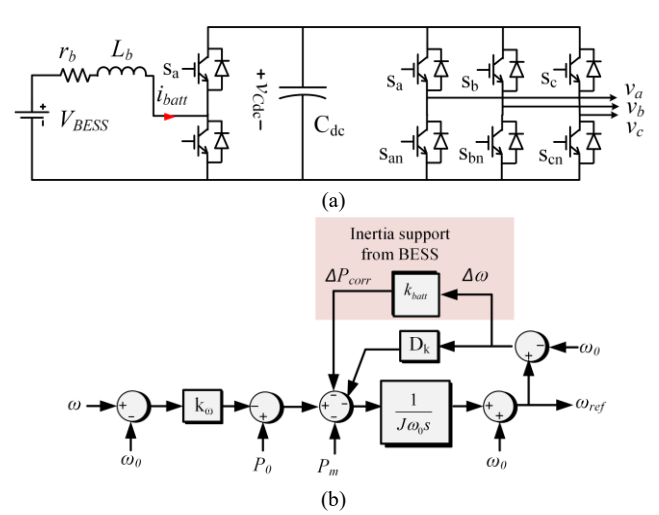


Fig. 5. BESS for the inertia support of LIPS: (a) BESS schematics, (b) modified VSG control to incorporate the BESS for the inertia emulation.

between the MPP and the PRM point is still an open challenge [38]. Moreover, this scheme can provide limited amount of VIE and this is highly dependent on the amount of available reserve active power [39]. AI-based frequency support and inertia emulation is presented in [40]. In this work, the role of the GFLs is redefined to provide the frequency support during the severe grid disturbances. The proposed approach uses artificial intelligence-based power reference correction (AI-PRC) module in the control of GFL inverter to provide fast frequency restoration and inertial support. The proposed scheme is highly adaptive to the network reconfigurations and as well as the type of disturbances. The AI based neural network is trained on both steady-state and the transient dynamics for the swing equation. Therefore, this provides the comprehensive dataset by analyzing all the feasible solutions of the swing equation to determine the amount of active power correction required to swiftly restore the grid frequency.

C. Other sources of inertia emulation for LIPS

The inertia for the LIPS can be emulated via various energy storage units. The energy storage units that can be employed for the inertia enhancement includes, capacitors, battery storage, flywheel, fuel cells, etc. The dc-link capacitors are required in the grid connected converters to provide harmonics filtering, reactive power compensation and voltage support. The similarity between the SG rotor and the dc-link capacitor can be formed by comparing it with the swing equation. The inertia constant for the dc-link capacitor [41] is given by,

$$H = \frac{C_{dc}V_{dcref}^{2}}{2S_{rated}} \tag{16}$$

where C_{dc} is the capacitance, V_{dcref} is the rated dc link voltage. The amount of VIE offered via dc-link capacitor is constrained by the maximum allowable voltage change ΔV_{dcref} , and the rated dc-link voltage [42]. Another scheme to provide the virtual inertia for supporting the system frequency of LIPS is utilizing battery energy storage system (BESS). Fig. 5 illustrates the schematics for the BESS incorporated with the three-phase inverter and the modified control of VSG with the BESS. The mechanism to provide the VIE via BES involves the calculation

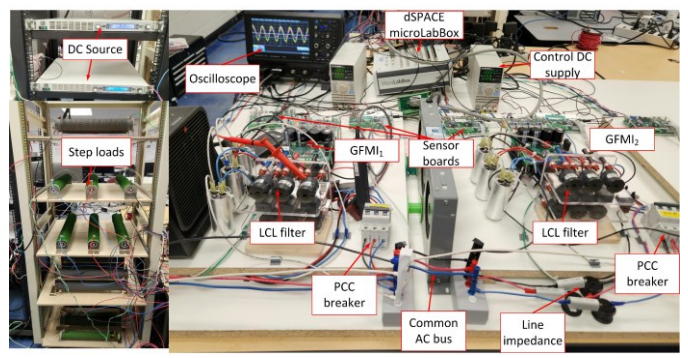


Fig. 6. Experimental setup to test the virtual inertia emulation from the grid forming inverters.

TABLE I: SYSTEM SPECIFICATIONS

Parameters	Value & units
Nominal power of GFMI ₁ , GFMI ₂	1.1 kW
Inverter-side filter inductor L_{11} , L_{12}	5 mH
Grid-side filter inductor L_{21} , L_{22}	3 mH
Filter Capacitor C_{fl} , C_{f2}	25 μF
Droop gain m	$0.5 \text{ x} 10^{-3} \text{ rad/s/W}$
Filter cut-off frequency ω_c	100 rad/s
Inertia constant for $VSG J$	2.2 kgm^2
DC Link voltage V_{dc}	300 V
Sampling time T_s	20 μs
Damping constant for VSG D_k	179.85 W/rad/s
Local loads R_{local}	22 Ohms
Step load R _{step}	30 Ohms

of the RoCoF in the event of the disturbance. Then, proportional to this RoCoF the corrective active power is supplied or stored to provide the inertial response to the frequency disturbance. The swing equation in (5) can be modified to incorporate the active power support provided from the BESS and it is given by,

$$J\frac{d\omega_{ref}}{dt} = P_0 - P_m - k_w(\omega_g - \omega_0) - D_k(\omega_{ref} - \omega_0) - \Delta P_{corr} \quad (17)$$

where, ΔP_{corr} is the active power supplied from the BES. The relation between the ΔP_{corr} and RoCoF is given as,

$$\Delta P_{corr} = k_{Batt} \frac{d\omega}{dt} \tag{18}$$

where, k_{Batt} is the battery constant that is derived based on the output power capacity of the battery. The equivalent inertia constant (H_{eq}) after incorporating the BES is given as,

$$H_{eq} = H + \frac{k_{Batt}}{2} \tag{19}$$

 $H_{eq} = H + \frac{k_{Batt}}{2} \tag{19}$ Therefore, the system inertia can be enhanced by modifying the k_{Batt} in (18). The BESS possess high energy density and faster response can be a good potential solution to provide the VIE for the LIPS. The works [16, 43] in explored the BESS for providing the fast inertia response for the frequency support of the LIPS during the severe disturbances. The BESS can help to reduce the negative effect of the intermittency of the renewable energy resources. However, measuring accurately the RoCoF is still a big challenge for incorporating the BESS [44]. Moreover, the batteries have inherent chemical issues that can jeopardize the system stability. A high-speed flywheel energy storage (FES) is another method that offers inertial support for the LIPS. The FES has a significantly higher flexibility in providing the high amount of active power in short periods (typically ranging from seconds to few minutes). This type of energy storage has a similar structure as the rotor of the SG has but it is rotating at very high speed. As FES is the rotating

structure it stores energy in form of kinetic energy, and it can be discharged at very high rate to provide the frequency support the grid during the severe disturbances. The inertia constant that FES model [45] includes is given as,

$$H = \frac{J_{FES}\omega_{\text{max}}^2}{2S_{rated}} \tag{20}$$

where, J_{FES} is the rotational inertia coefficient, ω_{max} is the maximum speed of rotation of FES, and S_{rated} is the rated apparent power for the flywheel. An adaptive VIE scheme is proposed [46] in the that uses the hysteresis based control scheme and can be easily integrated with the commercial FES systems. However, frequency support received from the flywheel lasts for few seconds and it relies on the secondary restoration system to fully restore system frequency of LIPS after the disturbance.

IV . EXPERIMENTAL RESULTS AND DISCUSSION ON VIE **SCHEMES**

The VIE schemes for the LIPS are compared via hardware implementation for two types of GFM control loops, namely, droop control and VSG control. The experimental setup used to test the VIE is depicted in Fig. 6. Moreover, the experimental setup specifications are given in the Table I and values of inertia constant and damping constant of VSG are selected by comparing it with a SG of similar power rating. In the setup, GFM₁ is controlled based on the VSG control and GFM₂ is controlled based on the droop-based controller. Both GFM inverters are operating in islanded mode and the breaker between GFM₁ and GFM₂ is open. Moreover, the model predictive control (MPC) scheme is utilized as an inner or level zero control to regulate the voltage and frequency according to reference generated from VSG and droop based GFM inverters. The GFM inverter that is controlled via droop scheme has a secondary controller like the frequency governor of VSG to restore frequency to nominal value after the load disturbance.

The VIE from both control is tested by adding the step load and varying the inertia constants. Specifically at instant t_1 the step load is added on the GFM₁. Fig. 7 (a) illustrates that the active power of the GFM₁ is increased from the 1.1 kW to 1.8 kW. The frequency response with different inertia constants (J) is illustrated in Fig. 7 (b). Specifically, with $\frac{1}{2}J$ the frequency has the lowest frequency nadir and the RoCoF was the largest. In case when inertia constant is J the frequency response improved as the frequency nadir improved and RoCoF decreased as compared to the case when inertia constant was ½J. Moreover, when the inertia constant was doubled the frequency nadir was the smallest and the RoCoF was the minimum. This case shows that inertia of the GFM is directly linked with inertia constant of the VSG control loop. In contrast the VIE from the droop control is illustrated in Fig. 7 (c)-(d). Specifically, at instant t_2 the step load is added, and the active power of the droop is changed from 1.1 kW to the 1.8 kW as depicted in the Fig. 7 (c). The frequency response to this load disturbance is illustrated in the Fig. 7 (d). Specifically, with different values of inertia constants the frequency response is improved. The frequency nadir is the lowest for the case with ½H and highest RoCoF was also recorded. As the inertia constant is changed to H and 2H the frequency nadir improves

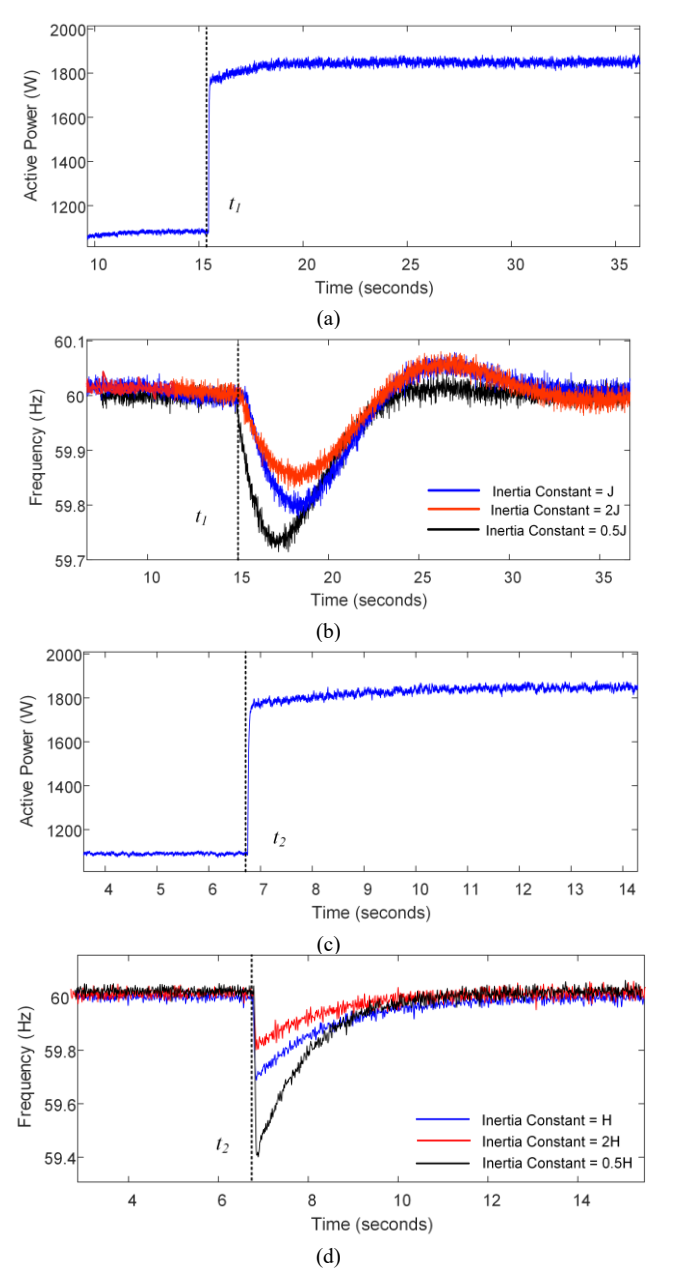


Fig. 7. Experimental results to show the VIE in response to the step-load; (a) active power of VSG, (b) frequency of VSG with different values of inertia constant, (c) active power of droop based GFM, and (d) frequency of droop based GFM with varying inertia constant.

and the RoCoF becomes smaller too. However, with droop a larger RoCoF was observed as compared to the VSG. Moreover, in the droop control with changing the value of inertia constant, the frequency nadir improves more as compared to the VSG.

IV. CONCLUSUION

This paper presented and compared different methods for the virtual inertia emulation for the low inertia power system. The implementation of these VIE methods for LIPS requires controller modifications and for some schemes additional hardware is needed. The frequency stability and the rotor angle stability that can be linked with the low inertia. However, with these VIE schemes the overall system inertia can be improved and the instability issues can be solved by boosting the system inertia. Specifically, in this work VIE is tested experimentally with two different GFM schemes, droop, and VSG. It is shown that by varying the inertia constants in the control loop the frequency response is improved by supporting the system inertia.

ACKNOWLEDGMENT

This work was supported by the U.S. National Science Foundation under Grant ECCS-2114442. The statements made herein are solely the responsibility of the author.

REFERENCES

- [1] B. K. Bose, "Global energy scenario and impact of power electronics in 21st century," *IEEE Transactions on Industrial Electronics*, vol. 60, no. 7, pp. 2638-2651, 2012.
- [2] O. Ellabban, H. Abu-Rub, and F. Blaabjerg, "Renewable energy resources: Current status, future prospects and their enabling technology," *Renewable and Sustainable Energy Reviews*, vol. 39, pp. 748-764, 2014.
- [3] A. M. Update, "Global wind report," Global Wind Energy Council, 2017.
- [4] N. I. B. R. P. Task, "Fast frequency response concepts and bulk power system reliability needs," NERC, p. 1, 2020.
- [5] Y. Su et al., "An adaptive PV frequency control strategy based on realtime inertia estimation," *IEEE Transactions on Smart Grid*, vol. 12, no. 3, pp. 2355-2364, 2020.
- [6] M. S. Alam, F. S. Al-Ismail, A. Salem, and M. A. Abido, "High-level penetration of renewable energy sources into grid utility: Challenges and solutions," *IEEE Access*, vol. 8, pp. 190277-190299, 2020.
- [7] T. Kerdphol, F. S. Rahman, and Y. Mitani, "Virtual inertia control application to enhance frequency stability of interconnected power systems with high renewable energy penetration," *Energies*, vol. 11, no. 4, p. 981, 2018.
- [8] S. Eftekharnejad, V. Vittal, G. T. Heydt, B. Keel, and J. Loehr, "Small signal stability assessment of power systems with increased penetration of photovoltaic generation: A case study," *IEEE transactions on* sustainable energy, vol. 4, no. 4, pp. 960-967, 2013.
- [9] D. Sampath Kumar, A. Sharma, D. Srinivasan, and T. Reindl, "Impact analysis of large power networks with high share of renewables in transient conditions," *IET Renewable Power Generation*, vol. 14, no. 8, pp. 1349-1358, 2020.
- [10] B. K. Poolla, D. Groß, and F. Dörfler, "Placement and implementation of grid-forming and grid-following virtual inertia and fast frequency response," *IEEE Transactions on Power Systems*, vol. 34, no. 4, pp. 3035-3046, 2019.
- [11] Q.-C. Zhong and G. Weiss, "Synchronverters: Inverters that mimic synchronous generators," *IEEE transactions on industrial electronics*, vol. 58, no. 4, pp. 1259-1267, 2010.
- [12] M. F. Umar, M. Hosseinzadehtaher, and M. B. Shadmand, "Enabling Aggregation of Heterogenous Grid-Forming Inverters via Enclaved Homogenization," *IEEE Access*, vol. 10, pp. 94765-94777, 2022, doi: 10.1109/ACCESS.2022.3204340.
- [13] A. Peña Asensio, F. Gonzalez-Longatt, S. Arnaltes, and J. L. Rodríguez-Amenedo, "Analysis of the converter synchronizing method for the contribution of battery energy storage systems to inertia emulation," *Energies*, vol. 13, no. 6, p. 1478, 2020.
- [14] Q. Peng, J. Fang, Y. Yang, T. Liu, and F. Blaabjerg, "Maximum Virtual Inertia From DC-Link Capacitors Considering System Stability at Voltage Control Timescale," *IEEE Journal on Emerging and Selected Topics in Circuits and Systems*, vol. 11, no. 1, pp. 79-89, 2021, doi: 10.1109/JETCAS.2021.3049686.
- [15] J. Yu, J. Fang, and Y. Tang, "Inertia Emulation by Flywheel Energy Storage System for Improved Frequency Regulation," in 2018 IEEE 4th Southern Power Electronics Conference (SPEC), 10-13 Dec. 2018 2018, pp. 1-8, doi: 10.1109/SPEC.2018.8635947.
- [16] G. Delille, B. Francois, and G. Malarange, "Dynamic frequency control support by energy storage to reduce the impact of wind and solar

- generation on isolated power system's inertia," *IEEE Transactions on sustainable energy*, vol. 3, no. 4, pp. 931-939, 2012.
- [17] N. Pogaku, M. Prodanovic, and T. C. Green, "Modeling, Analysis and Testing of Autonomous Operation of an Inverter-Based Microgrid," *IEEE Transactions on Power Electronics*, vol. 22, no. 2, pp. 613-625, 2007.
- [18] W. Du et al., "A comparative study of two widely used grid-forming droop controls on microgrid small-signal stability," *IEEE Journal of Emerging and Selected Topics in Power Electronics*, vol. 8, no. 2, pp. 963-975, 2019.
- [19] C. He, X. He, H. Geng, H. Sun, and S. Xu, "Transient stability of low-inertia power systems with inverter-based generation," *IEEE Transactions on Energy Conversion*, vol. 37, no. 4, pp. 2903-2912, 2022.
- [20] H. Bevrani, T. Ise, and Y. Miura, "Virtual synchronous generators: A survey and new perspectives," *International Journal of Electrical Power* & Energy Systems, vol. 54, pp. 244-254, 2014.
- [21] R. Rosso, S. Engelken, and M. Liserre, "Analysis of the behavior of synchronverters operating in parallel by means of component connection method (CCM)," in 2018 IEEE Energy Conversion Congress and Exposition (ECCE), 2018: IEEE, pp. 2228-2235.
- [22] Q.-C. Zhong, P.-L. Nguyen, Z. Ma, and W. Sheng, "Self-synchronized synchronverters: Inverters without a dedicated synchronization unit," *IEEE Transactions on power electronics*, vol. 29, no. 2, pp. 617-630, 2013
- [23] M. F. Umar, M. Hosseinzadehtaher, M. B. Shadmand, H. Livani, and M. Ben-Idris, "A Corrective Scheme to Prevent Adverse Dynamic Interaction of Grid-forming Inverters," in 2023 IEEE Power & Energy Society Innovative Smart Grid Technologies Conference (ISGT), 16-19 Jan. 2023 2023, pp. 1-5, doi: 10.1109/ISGT51731.2023.10066342.
- [24] A. G. Nazari, M. F. Umar, and M. B. Shadmand, "Optimal Synchronization Scheme of Grid-forming Inverters at Multiple Point of Coupling in Reconfiguring Grid," in 2023 IEEE Power & Energy Society General Meeting (PESGM), 16-20 July 2023 2023, pp. 1-5, doi: 10.1109/PESGM52003.2023.10252723.
- [25] D. Li, Q. Zhu, S. Lin, and X. Bian, "A self-adaptive inertia and damping combination control of VSG to support frequency stability," *IEEE Transactions on Energy Conversion*, vol. 32, no. 1, pp. 397-398, 2016.
- [26] M. F. Umar, M. Hosseinzadehtaher, and M. B. Shadmand, "Homogeneity Realization for Cluster of Heterogeneous Grid-forming Inverters," in 2021 6th IEEE Workshop on the Electronic Grid (eGRID), 8-10 Nov. 2021 2021, pp. 01-06, doi: 10.1109/eGRID52793.2021.9662145.
- [27] J. Liu, Y. Miura, and T. Ise, "Comparison of dynamic characteristics between virtual synchronous generator and droop control in inverterbased distributed generators," *IEEE Transactions on Power Electronics*, vol. 31, no. 5, pp. 3600-3611, 2015.
- [28] N. Soni, S. Doolla, and M. C. Chandorkar, "Inertia design methods for islanded microgrids having static and rotating energy sources," *IEEE Transactions on Industry Applications*, vol. 52, no. 6, pp. 5165-5174, 2016.
- [29] G. Raman and J. C. H. Peng, "Mitigating Stability Issues Due to Line Dynamics in Droop-Controlled Multi-Inverter Systems," *IEEE Transactions on Power Systems*, vol. 35, no. 3, pp. 2082-2092, 2020, doi: 10.1109/TPWRS.2019.2949311.
- [30] X. Wang, Y. W. Li, F. Blaabjerg, and P. C. Loh, "Virtual-impedance-based control for voltage-source and current-source converters," *IEEE Transactions on Power Electronics*, vol. 30, no. 12, pp. 7019-7037, 2014.
- [31] F. Guo, C. Wen, J. Mao, and Y. D. Song, "Distributed Secondary Voltage and Frequency Restoration Control of Droop-Controlled Inverter-Based Microgrids," *IEEE Transactions on Industrial Electronics*, vol. 62, no. 7, pp. 4355-4364, 2015, doi: 10.1109/TIE.2014.2379211.
- [32] L. Harnefors, M. Hinkkanen, U. Riaz, F. M. Rahman, and L. Zhang, "Robust analytic design of power-synchronization control," *IEEE Transactions on Industrial Electronics*, vol. 66, no. 8, pp. 5810-5819, 2018.
- [33] R. Rosso, X. Wang, M. Liserre, X. Lu, and S. Engelken, "Grid-forming converters: Control approaches, grid-synchronization, and future trends—A review," *IEEE Open Journal of Industry Applications*, vol. 2, pp. 93-109, 2021.
- [34] F. Zhao, X. Wang, and T. Zhu, "Low-frequency passivity-based analysis and damping of power-synchronization controlled grid-forming inverter," *IEEE Journal of Emerging and Selected Topics in Power Electronics*, vol. 11, no. 2, pp. 1542-1554, 2022.

- [35] R. Fu, X. Wang, Y. Zhang, and L. Li, "Inertial and primary frequency response of PLL synchronized VSC interfaced energy resources," *IEEE Transactions on Power Systems*, vol. 37, no. 4, pp. 2998-3013, 2021.
- [36] X. Guo et al., "Dynamic inertia evaluation for type-3 wind turbines based on inertia function," *IEEE Journal on Emerging and Selected Topics in Circuits and Systems*, vol. 11, no. 1, pp. 28-38, 2021.
- [37] A. F. Hoke, M. Shirazi, S. Chakraborty, E. Muljadi, and D. Maksimovic, "Rapid active power control of photovoltaic systems for grid frequency support," *IEEE Journal of Emerging and Selected Topics in Power Electronics*, vol. 5, no. 3, pp. 1154-1163, 2017.
- [38] B.-I. Crăciun, T. Kerekes, D. Séra, and R. Teodorescu, "Frequency support functions in large PV power plants with active power reserves," *IEEE Journal of Emerging and Selected Topics in Power Electronics*, vol. 2, no. 4, pp. 849-858, 2014.
- [39] E. I. Batzelis, G. E. Kampitsis, and S. A. Papathanassiou, "Power reserves control for PV systems with real-time MPP estimation via curve fitting," *IEEE Transactions on Sustainable Energy*, vol. 8, no. 3, pp. 1269-1280, 2017.
- [40] M. Hosseinzadehtaher, A. Zare, A. Khan, M. F. Umar, S. D'silva, and M. B. Shadmand, "AI-based Technique to Enhance Transient Response and Resiliency of Power Electronic Dominated Grids via Grid-Following Inverters," *IEEE Transactions on Industrial Electronics*, 2023.
- [41] E. Waffenschmidt and R. S. Hui, "Virtual inertia with PV inverters using DC-link capacitors," in 2016 18th European Conference on Power Electronics and Applications (EPE'16 ECCE Europe), 2016: IEEE, pp. 1-10
- [42] S. B. Karanki, N. Geddada, M. K. Mishra, and B. K. Kumar, "A DSTATCOM topology with reduced DC-link voltage rating for load compensation with nonstiff source," *IEEE Transactions on Power Electronics*, vol. 27, no. 3, pp. 1201-1211, 2011.
- [43] D. Gautam, L. Goel, R. Ayyanar, V. Vittal, and T. Harbour, "Control strategy to mitigate the impact of reduced inertia due to doubly fed induction generators on large power systems," *IEEE transactions on power systems*, vol. 26, no. 1, pp. 214-224, 2010.
- [44] D. Duckwitz and B. Fischer, "Modeling and design of \$ df/dt \$-based inertia control for power converters," *IEEE Journal of Emerging and Selected Topics in Power Electronics*, vol. 5, no. 4, pp. 1553-1564, 2017.
- [45] R. Pena-Alzola, D. Campos-Gaona, and M. Ordonez, "Control of flywheel energy storage systems as virtual synchronous machines for microgrids," in 2015 IEEE 16th Workshop on Control and Modeling for Power Electronics (COMPEL), 2015: IEEE, pp. 1-7.
- [46] S. Karrari, H. R. Baghaee, G. D. Carne, M. Noe, and J. Geisbuesch, "Adaptive inertia emulation control for high - speed flywheel energy storage systems," *IET generation, transmission & distribution*, vol. 14, no. 22, pp. 5047-5059, 2020.